

PAPER

ECG Biometric Authentication Using Deep CNN Feature Learning from Analytic Wavelet-Transformed Signals

Sairul Izwan Safie() , Noor Huda Ja'afar, Azyyati Johari, Mohd Anuar Ismail

Universiti Kuala Lumpur,
Johor Bahru, Malaysia

sairulizwan@unikl.edu.my

ABSTRACT

This paper investigates the use of continuous morse wavelet transform (CWT) coefficients as inputs to convolutional neural networks (CNNs) for electrocardiogram (ECG) biometric authentication. We evaluate the performance and generalization of pre-trained SqueezeNet architecture using the ECG-ID Database. Our approach involves extracting 10 scalograms from each subject's ECG signals and employing gradient descent optimization during training. The models demonstrate high accuracy, achieving over 90% on both training and validation datasets, indicating robust performance and minimal overfitting. Further analysis using the F1 confidence curve and ROC curve reveals a balanced trade-off between precision and recall, with an optimal F1 score of 0.84 and an AUC of 0.84, respectively. Additionally, we explore the impact of different CWT parameter settings, including Voice per Octave (VPO), symmetry parameter (γ), and time-bandwidth product (P^2). The optimal VPO of 41 yields an AUC of 0.87 and an F1 score of 0.84. The best performance is achieved with γ values greater than 2 and time-bandwidth products between 45 and 80, enhancing time localization and frequency resolution. In this study, the significance of fine-tuning wavelet parameters to improve the effectiveness of ECG biometric systems is demonstrated, demonstrating the potential of combining CWT and CNNs for reliable biometric authentication.

KEYWORDS

electrocardiogram (ECG), biometric, authentication, convolutional neural networks (CNNs), continuous morse wavelet transform (CWT)

1 INTRODUCTION

Virtual consultations, a form of telemedicine, enable online interactions between medical staff and patients. Its popularity has surged recently due to advancements in technology, particularly broadband and mobile diagnostics, extending telehealth services to patients' homes. These virtual consultations benefit patients and the healthcare system by facilitating remote communication and consultation [1]. They offer easy access to specialists around the clock without the need for appointments

Safie, S.I., Ja'afar, N.H., Johari, A., Ismail, M.A. (2024). ECG Biometric Authentication Using Deep CNN Feature Learning from Analytic Wavelet-Transformed Signals. *International Journal of Online and Biomedical Engineering (iJOE)*, 20(15), pp. 4–18. <https://doi.org/10.3991/ijoe.v20i15.51041>

Article submitted 2024-07-23. Revision uploaded 2024-08-26. Final acceptance 2024-10-21.

© 2024 by the authors of this article. Published under CC-BY.

and are generally cheaper than in-person visits, reducing out-of-pocket expenses. Cash-pay telemedicine services do not require insurance or referrals, providing healthcare access to uninsured individuals. Telemedicine also allows those in remote areas to consult doctors quickly, saving time and avoiding long trips, while keeping patients at home minimizes exposure to viruses and germs. Medical practitioners engaging in virtual primary care face several obstacles, including challenges related to digital exclusion, clinical uncertainty, delays in diagnosis and treatment, overuse and misuse of digital remote care, and incorrect association of medical records and treatments with individuals [2].

Electrocardiograms (ECGs) play a valuable role in virtual consultations by providing insights into heart rhythm, rate, and potential abnormalities. Clinicians can remotely monitor patients for arrhythmias, ischemia, and other cardiac conditions, helping to determine urgency and appropriate management [3]. Patients with cardiovascular conditions such as hypertension or heart failure can share ECG data during virtual visits, allowing clinicians to assess treatment effectiveness and adjust medications accordingly. Additionally, ECGs serve as a biometric authentication method, ensuring patient identity during virtual consultations.

2 RELATED WORK

An ECG or EKG is a quick and painless test that measures the electrical impulses of the heart, recording its electrical activity. Using ECGs for authentication or identification offers several advantages in enhancing security measures. ECGs provide a unique biometric trait due to their distinctiveness and stability over time. ECG patterns are specific to each person, making them a robust biometric identifier. Unlike external features such as fingerprints, ECGs are internal and harder to forge. ECG signals are difficult to replicate or manipulate, enhancing security in authentication scenarios. Additionally, ECG analysis confirms the subject's vitality during authentication, ensuring that the person is physically present and not using a static image or recording [4].

2.1 ECG features for biometric authentication

The categories of ECG features used for biometric authentication encompass various aspects of the ECG signal that uniquely identify individuals. Morphological features focus on the shape and structure of the ECG signal, capturing characteristics such as the P, Q, R, S, and T waves, and are commonly utilized for biometric authentication. Time interval features derive from the timing between specific points in the ECG signal, such as the duration of the PR interval, QRS complex, and QT interval, providing temporal information crucial for individual identification [5]. Amplitude features concentrate on the magnitude of specific components of the ECG signal, such as the height of the R wave or the depth of the S wave, capturing the intensity of certain signal components for authentication purposes. Frequency domain features involve analyzing the frequency components of the ECG signal using techniques such as Fourier analysis, offering insights into the spectral characteristics of the ECG signal and aiding in biometric identification. Some studies explore combined features, integrating morphological, time interval, and amplitude features to enhance the accuracy and robustness of ECG-based authentication systems [6]. Additionally, wavelet features apply wavelet transform techniques to the ECG signal to extract information at different scales, capturing both time and frequency domain characteristics for a comprehensive set of biometric authentication features [7].

2.2 Continuous morse wavelet transform for ECG biometric

Wavelet features are essential in ECG biometric authentication as they provide a comprehensive representation of the ECG signal in both time and frequency domains. Wavelet transforms are effective for analyzing non-stationary signals such as ECG due to their excellent time-frequency localization properties [8]. By decomposing the ECG signal using wavelet transforms, different frequency components at various scales can be extracted, enabling a detailed analysis of the signal. Matsuyama et al. [9] focused on applying wavelet decomposition to ECG signals to extract features such as normalized energy and entropy, laying the groundwork for utilizing wavelet transforms in ECG signal processing. Ingale et al. [10] explored using wavelet transforms to extract features for biometric authentication, highlighting the importance of wavelet coefficients in enhancing the accuracy of ECG-based identification systems. Ferdinando et al. [11] combined wavelet feature extraction methods, such as bivariate empirical mode decomposition (BEMD), with emotional data to improve the robustness and effectiveness of biometric systems. Ghoulmi et al. [12] investigated hybrid approaches combining wavelet transforms with other algorithms, such as the scale-invariant feature transform (SIFT), to leverage the strengths of different techniques for comprehensive feature extraction.

Analytic wavelets are complex-valued functions uniquely characterized by their one-sided frequency spectrum, confined to positive frequencies. This spectral property equips them to excel in the analysis of signals exhibiting time-varying amplitude and frequency modulations. Moreover, their capacity to pinpoint localized discontinuities makes them indispensable tools for various signal processing applications. One of their key properties is having a null Fourier transform for negative frequencies, resulting in one-sided spectra. This characteristic is advantageous for time-frequency analysis using the continuous wavelet transform, which provides phase information through complex-valued coefficients. Various categories of analytic wavelets include generalized morse wavelets (GMWs) [13], airy wavelets [14], analytic derivative of Gaussian wavelets, and cauchy wavelets [15].

Generalized morse wavelets provide several advantages due to their distinctive properties:

- Analytic properties: GMWs are truly analytic wavelets with Fourier transforms supported only on the positive real axis, making them ideal for analyzing modulated signals with time-varying amplitude and frequency.
 - Parameterized flexibility: GMWs have two adjustable parameters, symmetry (γ) and time-bandwidth product (P^2), allowing for the customization of wavelet properties and behaviors. Many commonly used analytic wavelets are special cases of generalized Morse wavelets.
- Phase information: GMWs encode phase information in their complex wavelet coefficients, which is valuable for various signal processing tasks, including classification and interpretation. This phase of information enhances their utility in different applications.

2.3 Convolutional neural network for ECG biometric authentication

The use of convolutional neural networks (CNNs) for biometric applications has advanced significantly, leveraging deep learning for accurate and reliable identification. Genovese et al. [16] introduced PalmNet, a method using Gabor-PCA convolutional networks for touchless palmprint recognition. This approach

effectively handles variations in scale, rotation, and illumination by extracting highly discriminative features. Additionally, Sedik et al. [17] employed CNNs for biometric alteration detection in secure smart cities, illustrating the application of deep learning techniques to enhance security in 5G network-based environments.

Liu et al. [18] expanded the field of ECG biometric authentication with a cascaded CNN (CCNN) approach for feature extraction and biometric comparison of ECG heartbeats. Similarly, Hammad et al. [19] focused on multimodal biometric systems, using CNNs to fuse ECG and fingerprint data for secure authentication. Ingale et al. [10] explored the impact of filtering, segmentation, feature extraction, and health status on ECG authentication, while Rehman et al. [20] enhanced the matching process by employing CNNs to binarize ECG signals.

Alduwaile and Islam [21] demonstrated the effectiveness of using CNNs for ECG biometric recognition with a single heartbeat, showcasing the potential for developing reliable ECG-based systems. Rahman et al. [22] compared unimodal and multimodal systems incorporating deep learning and traditional methods, particularly in the context of fingerprint and ECG signal fusion. Jomaa et al. [23] developed an end-to-end CNN-based multimodal system for integrating ECG and fingerprint data. Chan et al. [24] further advanced the field by creating a phase space reconstruction (PSR)-based CNN to improve identification accuracy.

2.4 Contributions

This study aims to enhance ECG biometric authentication by addressing key challenges in feature extraction and model performance. Previous works in this field have often relied on traditional feature extraction methods or computationally intensive models, which may not be suitable for resource-constrained environments. The gap in the literature lies in the lack of exploration of wavelet-based methods for improving feature extraction in lightweight CNN architectures. Our study introduces the use of CWT filter bank coefficients for ECG signal processing, providing a novel approach to feature extraction that is both efficient and effective. We evaluate ShuffleNet, a low-memory CNN architecture, which is more appropriate for devices with limited resources. Furthermore, we investigate the impact of different wavelet parameter settings on system performance, optimizing for metrics such as accuracy, AUC, F1 score, and EER. The novelty of this study is demonstrated through a comprehensive analysis of the proposed approach using the ECG-ID database, which is known for its challenging nature. The results show significant improvements in biometric identification accuracy and generalization, thus advancing the state of ECG-based biometric technologies.

3 SIMULATION SETUP

3.1 ECG ID database

The ECG-ID Database is a collection of 310 ECG recordings gathered from 90 individuals for the purpose of developing biometric identification systems based on ECG signals. Contributed by Tatiana Lugovaya as part of her master's thesis, the database consists of 20-second ECG recordings captured from lead I, digitized at a sampling rate of 500 Hz with 12-bit resolution [25]. Each recording includes annotations for 10 heartbeats, marked by R- and T-wave peaks, which were automatically detected. Supplementary demographic information, such as age, gender, and recording date,

is provided in accompanying header files. The database encompasses a diverse group of 44 men and 46 women ranging in age from 13 to 75 years, primarily composed of students, colleagues, and acquaintances of the author. It's important to note that the raw ECG signals are contaminated with both high- and low-frequency noise. The database can be accessed for download from the PhysioNet website [26].

Most individuals in the database have at least two ECG recordings, each with a duration of 10,000 samples. For this study, we utilized the first two recordings from each individual. Each ECG signal was segmented into four parts of 2,500 samples, resulting in eight segments per individual. Of these, 60% were used for training, and the remaining 40% for testing. The ECG signals were then transformed into time-frequency representations known as scalograms, which are the absolute values of the CWT coefficients. To generate these scalograms, a precomputed CWT filter bank was used, optimizing the process for multiple signals with consistent parameters. The resulting 2D RGB scalograms served as input to the CNN for biometric authentication.

3.2 SqueezeNet

SqueezeNet is a deep neural network for computer vision developed by Forrest N. Iandola, Matthew W. Moskewicz, Khalid Ashraf, Song Han, William J. Dally, and Kurt Keutzer at DeepScale, University of California, Berkeley, and Stanford University [27]. Initially released in 2016, SqueezeNet is designed as a compact CNN architecture with several advantages that make it suitable for various applications, including scenarios with limited resources. The SqueezeNet architecture uses three key strategies to reduce parameter size while maintaining high accuracy:

- 1×1 Filters: Replaces conventional 3×3 filters with 1×1 filters, reducing the number of parameters by about nine times. This effectively captures relationships among channels.
- Squeeze Layer: Reduces the number of input channels to 3×3 filters by preceding them with 1×1 filters, decreasing computational complexity and memory requirements.
- Late Downsampling: Delays downsampling until later in the network to create larger feature maps, improving classification accuracy with the same number of parameters.

The architecture includes a standalone convolutional layer (conv1), eight Fire modules (fire2–fire9), and a final convolutional layer (conv10) as shown in Figure 1 [28].

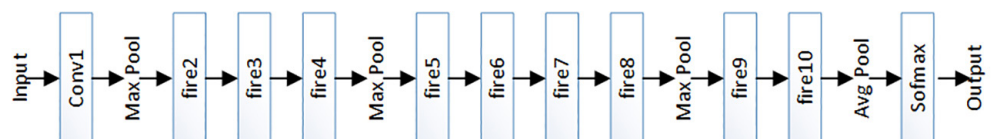


Fig. 1. SqueezeNet architecture

Each Fire module is composed of a squeeze layer with only 1×1 filters and an expand layer that contains a mix of 1×1 and 3×3 convolution filters, as shown in Figure 2. Importantly, the number of filters in the squeeze layer is kept smaller than in the expand layer. The number of filters per Fire module gradually increases from the beginning to the end of the network.

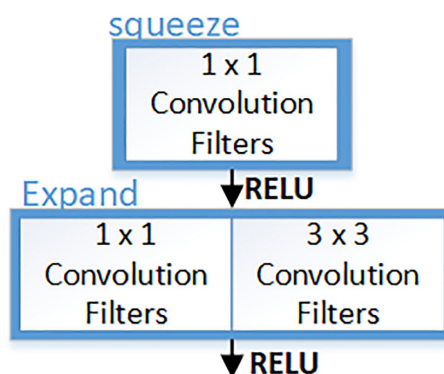


Fig. 2. Fire module

Max-pooling with a stride of 2 is performed after layers conv1, fire4, and fire8. After layer conv10, average-pooling is applied, resulting in a flattened vector with dimensions equal to the number of classes. This vector is then fed into the SoftMax layer for classification. Notably, SqueezeNet does not employ fully connected layers, which drastically reduces the number of parameters in the model. To mitigate overfitting, a dropout with a ratio of 50% is applied after the fire9 module, providing regularization during training.

3.3 Performance matrix

In CNNs for classification tasks, the performance matrix is essential for evaluating model effectiveness. Various metrics, such as output classification accuracy and F1-score, are commonly used. Confusion matrices are also employed to analyze the decision-making process and overall performance of CNN models. Similarly, the evaluation of biometric systems frequently involves confusion matrices to scrutinize the system's decision-making and performance.

Classification accuracy and validation loss. Accuracy, a conventional metric in machine learning, quantifies a model's predictive capability by determining the ratio of correct to total predictions. While seemingly straightforward, accuracy can be misleading, especially when dealing with imbalanced datasets or scenarios where the costs of false positives and negatives differ significantly. For instance, in medical diagnosis, a false negative, indicating a missed disease, carries far graver consequences than a false positive, a misdiagnosed condition.

To complement accuracy, validation loss provides a measure of a model's generalization ability. This metric quantifies the discrepancy between a model's predicted outputs and ground truth values within a holdout dataset. A lower validation loss typically signifies better model performance on unseen data. The selection of an appropriate loss function is critical. Mean squared error is commonly employed for regression tasks, while binary cross-entropy is suitable for binary classification problems.

Confusion matrix. A confusion matrix offers a granular assessment of a classification model's performance by tabulating the alignment between predicted and actual class labels. As illustrated in Figure 3, this matrix is indispensable for evaluating model accuracy and reliability. This tabular representation is indispensable for evaluating model accuracy and reliability. A true positive occurs when both the actual and predicted classes are positive, indicating correct model identification. Conversely, a false negative arises when the actual class is positive but the model incorrectly predicts it as negative, signifying a model failure to recognize the positive class. A false positive emerges when the actual class is negative, yet the model erroneously predicts it as positive, highlighting incorrect identification. Finally, a

true negative signifies the correct classification of a negative instance. Through a meticulous analysis of these components, practitioners can gain profound insights into model strengths and weaknesses.

	PREDICTED POSITIVE	PREDICTED NEGATIVE
ACTUAL POSITIVE	TRUE POSITIVE	TRUE NEGATIVE
ACTUAL NEGATIVE	FALSE POSITIVE	FALSE NEGATIVE

Fig. 3. Confusion matrix

F1-score. The F1 score offers a comprehensive evaluation of a model's performance by incorporating both precision and recall. Precision measures the proportion of correctly predicted positive instances out of all instances predicted as positive, while recall (also known as sensitivity) calculates the proportion of correctly predicted positive instances out of all actual positive instances.

$$Precision = \frac{TP}{TP + FP} \quad (1)$$

$$Recall = \frac{TP}{TP + FN} \quad (2)$$

$$F1 = \frac{2 \times Precision \times Recall}{Precision + Recall} \quad (3)$$

The F1 score constitutes a balanced metric that harmonizes precision and recall, offering a comprehensive appraisal of model performance. By averaging precision and recall using the harmonic mean, the F1 score penalizes extreme values and rewards models that excel in both identifying true positives and minimizing false positives and negatives. This is especially advantageous in scenarios with imbalanced class distributions, where accuracy alone may be misleading. A higher F1 score signifies a superior balance between precision and recall, indicating a more robust model capable of accurately classifying instances across both classes.

Receiver operating characteristics (ROC) curves. Receiver operating characteristic (ROC) curves are essential tools for evaluating the performance of classification models, especially in scenarios where balancing the true positive rate (sensitivity) and the false positive rate (FPR) (1-specificity) is critical.

$$True\ Positive\ Rate = \frac{TP}{TP + FN} \quad (4)$$

$$False\ Positive\ Rate = \frac{FP}{FP + TN} \quad (5)$$

These curves provide a graphical representation of the trade-off between sensitivity and specificity as the discrimination threshold of a classifier is varied.

The area under the curve (AUC) metric, derived from the ROC curve, offers a comprehensive assessment of a classifier's overall performance. A higher AUC signifies superior discriminative capability between positive and negative classes. In tandem, the ROC curve provides invaluable insights into a model's diagnostic efficacy, making these metrics essential tools for evaluating classification models. The equal error rate (EER), another pivotal metric, identifies the ROC curve point where false positives and false negatives are equalized. This threshold signifies the classifier's balance between accepting and rejecting instances. A lower EER indicates a more reliable and accurate model.

4 RESULTS AND DISCUSSION

4.1 Robustness and generalization of the model

Our initial simulation evaluates the robustness and generalization of the model for ECG biometric authentication. We used the entire ECG-ID Database, extracting 10 scalograms from the ECG of each subject. 70% of the scalograms were allocated for training, with the remaining 30% for validation. A pre-trained SqueezeNet model was utilized, with training conducted using a gradient descent algorithm to minimize the loss function. The initial learning rate was set to 0.0003, with a batch size of 10, and training was performed over 50 epochs.

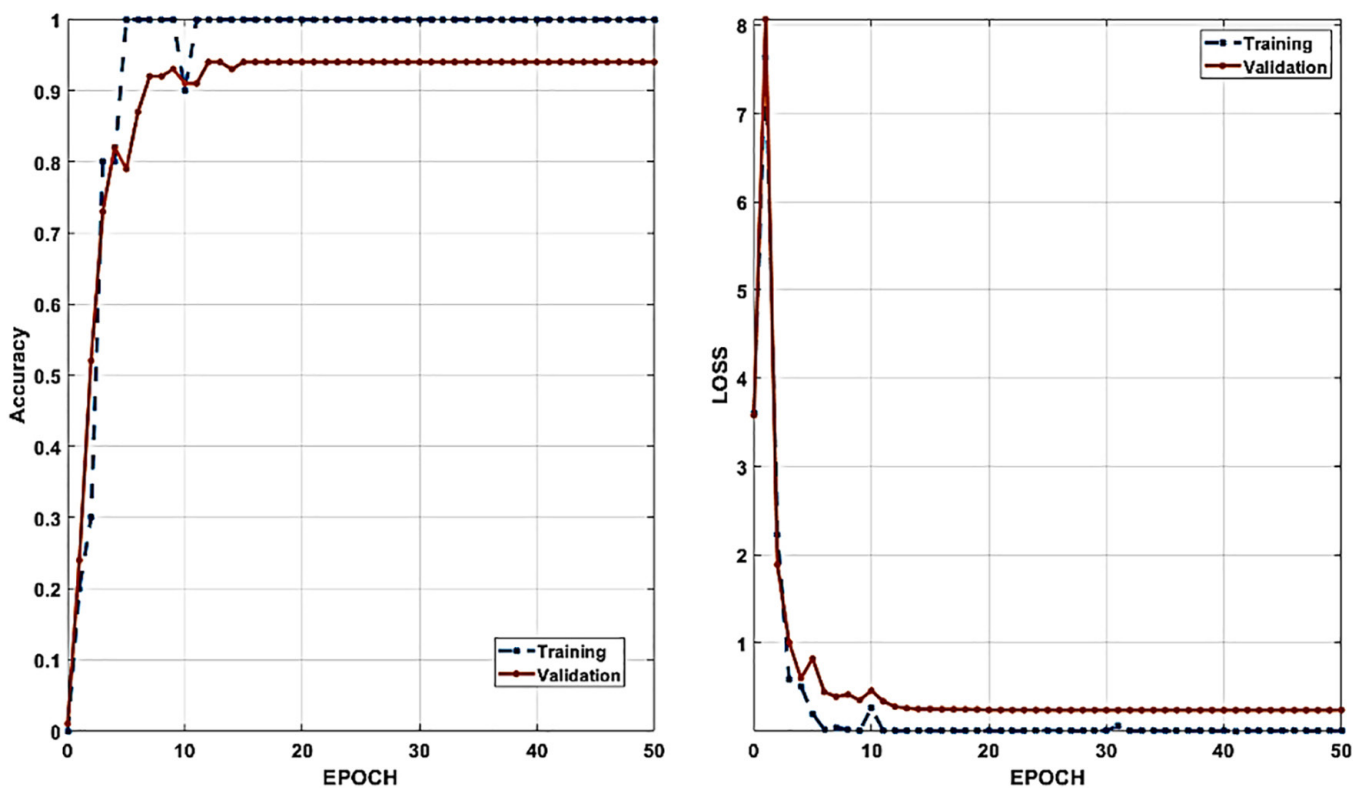


Fig. 4. Training and validation results

Figure 4 illustrates the accuracy and loss performance for both the training and validation datasets. From the 15th epoch onward, validation accuracy and loss stabilized at 0.94 and 0.25, respectively. Training accuracy reached one, and training loss dropped to 0 from the 15th epoch onward. These results indicate that both training and validation accuracies exceeded 0.9, suggesting the model performs well on both seen and unseen data. The minimal difference between training accuracy and validation accuracy (less than 0.1) suggests the model is not overfitting. The near-zero training loss indicates the model effectively fits the training data, while the low validation loss demonstrates good generalization to new and unseen data.

4.2 Performance across different decision thresholds

Our next evaluation examines the model's performance across various decision thresholds, focusing on the balance between precision and recall as indicated by the F1 confidence curve shown in Figure 5. As illustrated, most thresholds yield satisfactory F1 scores around 0.68. The F1 score improves from a threshold value of 0.6, reaching its peak at 0.84 with a threshold value of 0.998.

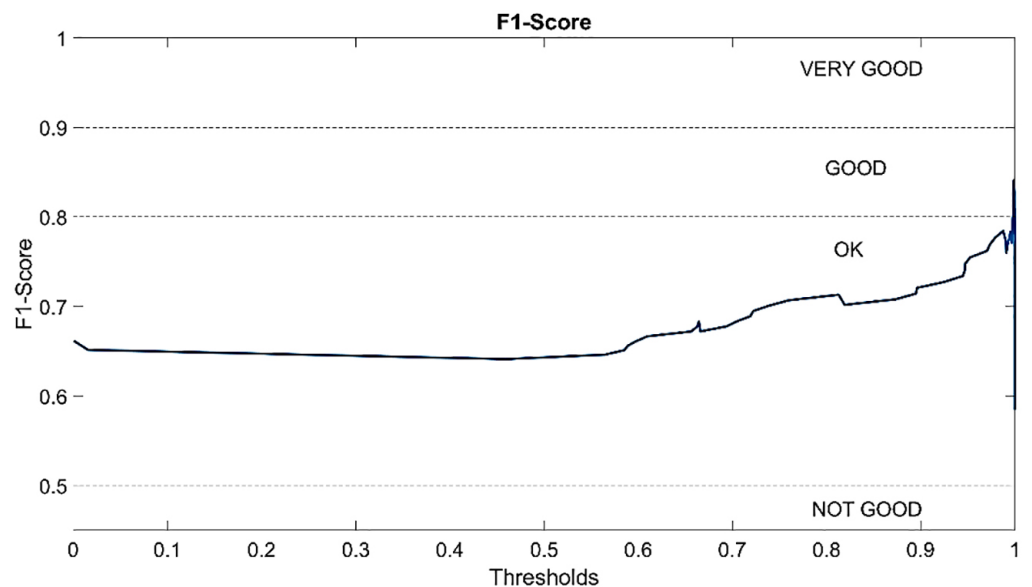


Fig. 5. F1-Confidence curve

These results indicate that the model performs consistently well across a range of thresholds, but the optimal performance is achieved at a specific high threshold value. The initial satisfactory F1 scores around 0.68 suggest that the model maintains a reasonable balance between precision and recall across different decision points. As the threshold value increases, the model becomes more stringent in classifying positive instances, which improves the precision and recall balance, leading to a higher F1 score.

The peak F1 score of 0.84 at a threshold value of 0.998 signifies that the model achieves the best trade-off between precision and recall at this point. This high threshold value indicates that the model is very selective in predicting positive instances, minimizing false positives while still correctly identifying a significant number of true positives. Consequently, this suggests that the model is highly effective

at distinguishing between classes when applying a stringent decision threshold, resulting in a more reliable biometric authentication system.

4.3 Verification through ROC analysis

To further validate our previous analysis, we examine the trade-off between true positive rate (TPR or sensitivity) and FPR as the decision threshold varies, based on the ROC curves shown in Figure 6. The ROC curve is close to the top-left corner, with an AUC of 0.85, indicating that the trained model is highly effective for biometric authentication.

Additionally, the EER is 0.165 at a threshold value of 0.998. The EER represents the point where the false acceptance rate equals the false rejection rate, indicating a balanced trade-off between the two types of errors. An AUC of 0.84 and low EER confirm that the model maintains robust performance across different thresholds, ensuring a high level of reliability and accuracy in identifying individuals based on their ECG signals.

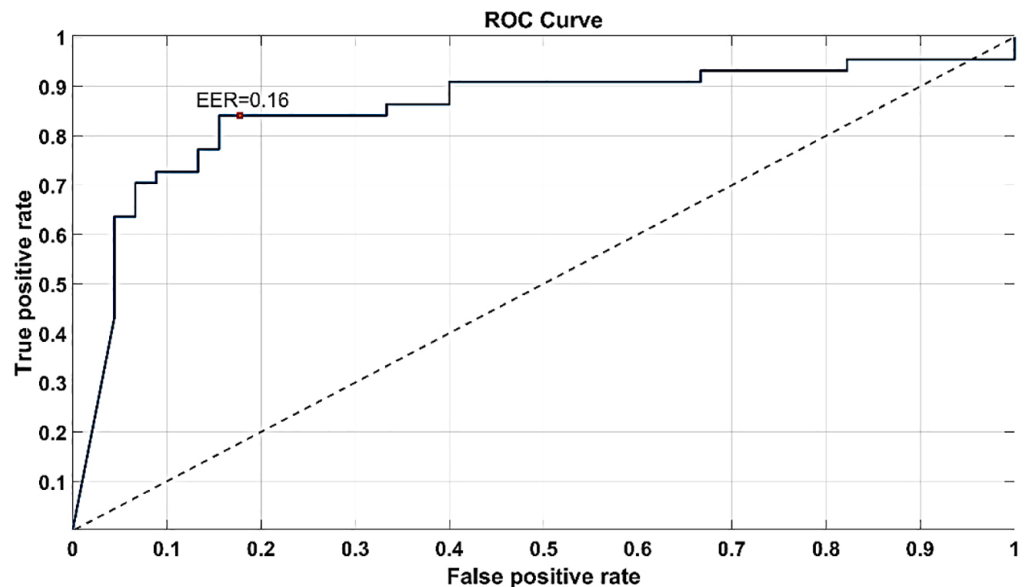


Fig. 6. ROC curves

4.4 Performance with CWT parameters

We further evaluated the system's performance using various CWT parameter settings. The CWT decomposes a signal into different scales (frequencies) using wavelet functions, where the scale parameter controls the width of the wavelet function—larger scales correspond to lower frequencies and smaller scales correspond to higher frequencies. In performing the CWT, the discretization of the scale parameter significantly affects the number of wavelet filters used. “Voices per Octave” (VPO) refers to the number of wavelet filters per octave, specifying how many intermediate scales are used between each octave.

Our evaluation tested VPO values ranging from one to 45 for the ECG biometric system. As illustrated in Figure 7, the optimal VPO for the proposed system is 41,

achieving an AUC of 0.87, an F1 Score of 0.84, and an EER of 0.18. When VPO is greater than five, the system maintains an average F1 score of 0.79, an average AUC of 0.79, and an average EER of 0.26.

These results suggest that a higher VPO, particularly around 41, enhances the system's ability to accurately and reliably authenticate individuals using ECG signals. The improved metrics at higher VPO values indicate that a finer discretization of the scale parameter allows the model to capture more detailed frequency information, thus enhancing its performance.

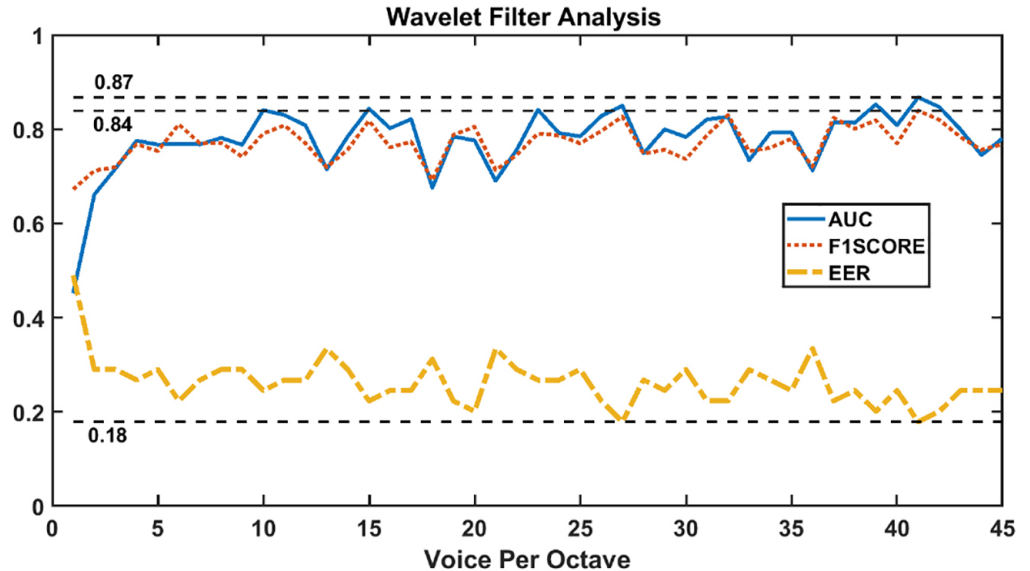


Fig. 7. Evaluation of system performance across different voices per octave (VPO) settings

In addition to VPO, the symmetry parameter (γ) and time-bandwidth product (P^2) are crucial Morse wavelet parameters that influence the system's performance. Figure 8 illustrates system performance in terms of accuracy, AUC, F1-Score, and EER across various settings of these parameters. The results indicate optimal performance with a symmetry parameter greater than two and a time-bandwidth product between 45 and 80.

The symmetry parameter controls the wavelet's symmetry in time, effectively demodulating skewness. A common recommendation is to use a moderate value of γ around three, which balances time localization and frequency resolution, minimizing skewness while maintaining a reasonable time bandwidth product. The time bandwidth product (P^2) is proportional to the wavelet duration in time, determining how many oscillations fit into the wavelet's center window. A higher P^2 provides better frequency resolution, capturing fine details in the ECG signal but resulting in longer duration in the time domain. Conversely, a lower P^2 enhances time localization, allowing for precise event detection.

These results highlight the importance of carefully selecting wavelet parameters to optimize the performance of ECG biometric systems. The findings suggest that a symmetry parameter greater than two and a time-bandwidth product between 45 and 80 achieve the best balance between frequency resolution and time localization, thereby enhancing the overall accuracy and reliability of biometric authentication.

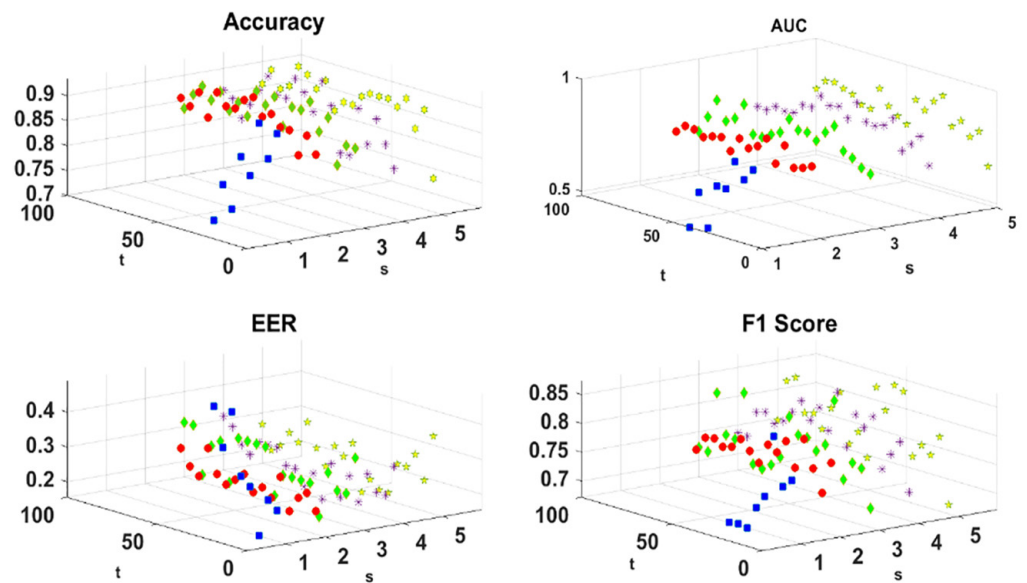


Fig. 8. Performance metrics (accuracy, AUC, F1-Score, EER) for different combinations of symmetry parameter (γ) and time-bandwidth product (P^2)

5 CONCLUSION

This study demonstrates the effectiveness of using CWT coefficients as inputs to CNNs for ECG biometric authentication. Through comprehensive simulations and evaluations, we established the robustness, generalization, and optimal parameter settings of our model.

In the initial simulation using the ECG-ID Database, the model showed strong robustness and generalization capabilities. By training a pre-trained SqueezeNet model on a diverse dataset and using gradient descent with a batch size of 10 and an initial step size of 0.0003, we achieved high training and validation accuracies, both exceeding 0.9, with minimal overfitting. The near-zero training loss and low validation loss affirmed the model's strong generalization to unseen data. Exploring performance across different decision thresholds, the F1 confidence curve highlighted a balance between precision and recall, peaking at an F1 score of 0.84 with a threshold value of 0.998. ROC curve analysis further confirmed high performance with an AUC of 0.84 and an EER of 0.16, indicating a reliable model.

Evaluating different CWT parameter settings, specifically the voice per octave (VPO), revealed that a VPO of 41 yielded the best results with an AUC of 0.87, an F1 score of 0.84, and an EER of 0.18. Higher VPO values consistently improved performance, with average F1 scores and AUC around 0.79 and an average EER of 0.26. Further investigation into morse wavelet parameters, namely the symmetry parameter (γ) and time-bandwidth product (P^2), showed optimal performance with γ greater than two and a time-bandwidth product between 45 and 80. These settings balance time localization and frequency resolution, optimizing wavelet capabilities.

Based on our findings, we recommend focusing on fine-tuning the CWT parameters and hyperparameters of CNNs to achieve optimal performance. Specifically, adjusting the VPO and parameters such as symmetry and time-bandwidth product can significantly impact the accuracy and reliability of biometric systems. Researchers should also consider leveraging pre-trained models and gradient descent

algorithms for effective training and evaluation. Additionally, thorough experimentation with decision thresholds and performance metrics, such as F1 score, AUC, and EER, is essential for developing robust biometric authentication systems. These practices can guide future work in optimizing ECG-based authentication models and advancing the field.

6 REFERENCES

- [1] S. Liew, V. Pallath, Y. Rasali, C. C. Foong, W. Hong, and M. Tan, "Knowledge, attitude, and practice of virtual consultation among outpatients at a teaching hospital in Malaysia," *PLoS One*, vol. 18, no. 12, p. e0289176, 2023. <https://doi.org/10.1371/journal.pone.0289176>
- [2] E. Li *et al.*, "General practitioners' perceptions of using virtual primary care during the COVID-19 pandemic: An international cross-sectional survey study," *PLOS Digital Health*, vol. 1, no. 5, p. e0000029, 2022. <https://doi.org/10.1371/journal.pdig.0000029>
- [3] M. Takami *et al.*, "Telehealth follow-up using a real-time electrocardiogram device improves electrocardiogram monitoring duration and patient satisfaction after catheter ablation," *Circulation Reports*, vol. 5, no. 11, pp. 415–423, 2023. <https://doi.org/10.1253/circrep.CR-23-0083>
- [4] S. Safie, J. Soraghan, and L. Petropoulakis, "Electrocardiogram (ECG) biometric authentication using Pulse Active Ratio (PAR)," *Information Forensics and Security*, vol. 6, no. 4, pp. 1315–1322, 2011. <https://doi.org/10.1109/TIFS.2011.2162408>
- [5] L. Biel, O. Pettersson, L. Philipson, and P. Wide, "ECG analysis: A new approach in human identification," *IEEE Transactions on Instrumentation and Measurement*, vol. 50, no. 3, pp. 808–812, 2001. <https://doi.org/10.1109/19.930458>
- [6] A. Kailas and G. Murthy, "Deep learning based biometric authentication using electrocardiogram and iris," *IAES International Journal of Artificial Intelligence (IJ-AI)*, vol. 13, no. 1, p. 1090–1103, 2024. <https://doi.org/10.11591/ijai.v13.i1.pp1090-1103>
- [7] S. S. Mahmoud and J. Jusak, "Wavelets in ECG security application," in *Wavelet Theory and Its Applications*, S. Radhakrishnan, Ed., IntechOpen, 2018. <https://doi.org/10.5772/intechopen.74477>
- [8] M. Bogdanov, D. Nasyrov, I. Dumchikova, and A. Samigullin, "Processing of biomedical data with machine learning," in *Proceedings of the 21st International Workshop on Computer Science and Information Technologies (CSIT 2019)*, Atlantis Press, pp. 6–16, 2019. <https://doi.org/10.2991/csit-19.2019.2>
- [9] A. Matsuyama and M. Jonkman, "The application of wavelet and feature vectors to ECG signals," *Australasian Physical & Engineering Sciences in Medicine*, vol. 29, 2006. <https://doi.org/10.1007/BF03178823>
- [10] M. Ingale, R. Cordeiro, S. Thentu, Y. Park, and N. Karimian, "ECG biometric authentication: A comparative analysis," *IEEE Access*, vol. 8, pp. 117853–117866, 2020. <https://doi.org/10.1109/ACCESS.2020.3004464>
- [11] H. Ferdinando, T. Seppänen, and E. Alasaarela, "Bivariate empirical mode decomposition for ECG-based biometric identification with emotional data," in *2017 39th Annual International Conference of the IEEE Engineering in Medicine and Biology Society (EMBC)*, 2017, pp. 450–453. <https://doi.org/10.1109/EMBC.2017.8036859>
- [12] L. Ghoualmi, A. Draa, and S. Chikhi, "Ear feature extraction using a DWT-SIFT hybrid," in *Intelligent Data Analysis and Applications, Advances in Intelligent Systems and Computing*, A. Abraham, X. Jiang, V. Snášel, and J. S. Pan, Eds., vol. 370, 2015, pp. 37–47. https://doi.org/10.1007/978-3-319-21206-7_4

- [13] T. L. Leise, "Analysis of nonstationary time series for biological rhythms research," *Journal of Biological Rhythms*, vol. 32, no. 3, pp. 187–194, 2017. <https://doi.org/10.1177/0748730417709105>
- [14] S. Ortuño-Miró, S. Molina-Rodríguez, C. Belmonte, and J. Ibañez-Ballesteros, "Identifying ADHD boys by very-low frequency prefrontal fNIRS fluctuations during a rhythmic mental arithmetic task," *Journal of Neural Engineering*, vol. 20, no. 3, pp. 1–23, 2023. <https://doi.org/10.1088/1741-2552/acad2b>
- [15] M. Walencykowska and A. Kawalec, "Application of Continuous Wavelet Transform and Artificial Neural Network for Automatic Radar Signal Recognition," *Sensors*, vol. 22, no. 19, p. 7434, 2022. <https://doi.org/10.3390/s22197434>
- [16] A. Genovese, V. Piuri, K. N. Plataniotis, and F. Scotti, "PalmNet: Gabor-PCA convolutional networks for touchless Palmprint recognition," *IEEE Transactions on Information Forensics and Security*, vol. 14, no. 12, pp. 3160–3174, 2019. <https://doi.org/10.1109/TIFS.2019.2911165>
- [17] A. Sedik *et al.*, "Deep learning modalities for biometric alteration detection in 5G networks-based secure smart cities," *IEEE Access*, vol. 9, pp. 94780–94788, 2021. <https://doi.org/10.1109/ACCESS.2021.3088341>
- [18] L. Xiaoyu, "Application and research of artificial intelligence in mechatronic engineering," in *2020 5th International Conference on Mechanical, Control and Computer Engineering (ICMCCE)*, 2020, pp. 235–238. <https://doi.org/10.1109/ICMCCE51767.2020.00059>
- [19] M. Hammad, Y. Liu, and K. Wang, "Multimodal biometric authentication systems using Convolution Neural Network based on different level fusion of ECG and fingerprint," *IEEE Access*, vol. 7, pp. 26527–26542, 2018. <https://doi.org/10.1109/ACCESS.2018.2886573>
- [20] Z. u. Rehman, S. Altaf, S. Ahmad, M. Alqahtani, S. Huda, and S. Iqbal, "Advanced authentication scheme with bio-key using Artificial Neural Network," *Sustainability*, vol. 14, no. 7, p. 3950, 2022. <https://doi.org/10.3390/su14073950>
- [21] D. A. AlDuwaile and M. S. Islam, "Using convolutional neural network and a single heartbeat for ECG biometric recognition," *Entropy*, vol. 23, no. 6, p. 733, 2021. <https://doi.org/10.3390/e23060733>
- [22] S. Rahman and A. Alluhaidan, "Enhanced multimodal biometric recognition systems based on deep learning and traditional methods in smart environments," *PLoS One*, vol. 19, no. 2, p. e0291084, 2024. <https://doi.org/10.1371/journal.pone.0291084>
- [23] R. M. Jomaa, H. Mathkour, Y. Bazi, and M. S. Islam, "End-to-end deep learning fusion of fingerprint and electrocardiogram signals for presentation attack detection," *Sensors*, vol. 20, no. 7, p. 2085, 2020. <https://doi.org/10.3390/s20072085>
- [24] H.-L. Chan, H.-W. Chang, W.-Y. Hsu, P.-J. Huang, and S.-C. Fang, "Convolutional neural network for individual identification using phase space reconstruction of electrocardiogram," *Sensors*, vol. 23, no. 6, p. 3164, 2023. <https://doi.org/10.3390/s23063164>
- [25] T. S. Lugovaya, "Biometric human identification based on electrocardiogram," Faculty of Computing Technologies and Informatics, Electrotechnical University "LETI", Saint-Petersburg, Russian Federation, 2005.
- [26] A. Goldberger *et al.*, "PhysioBank, PhysioToolkit, and PhysioNet: Components of a new research resource for complex physiologic signals," *Circulation*, vol. 101, no. 23, pp. e215–e220, 2000. <https://doi.org/10.1161/01.CIR.101.23.e215>
- [27] F. Iandola, S. Han, M. Moskewicz, K. Ashraf, W. Dally, and K. Keutzer, "SqueezeNet: AlexNet-level accuracy with 50x fewer parameters and <0.5MB model size," *arXiv pre-print arXiv:1602.07360*, 2016. <https://doi.org/10.48550/arXiv.1602.07360>
- [28] S. I. Safie, N. S. A. Kamal, E. M. M. Yusof, M. Z.-W. M. Tohid, and N. H. Jaafar, "Comparison of SqueezeNet and DarkNet-53 based YOLO-V3 Performance for Beehive Intelligent Monitoring System," in *2023 IEEE 13th Symposium on Computer Applications & Industrial Electronics (ISCAIE)*, 2023, pp. 62–65. <https://doi.org/10.1109/ISCAIE57739.2023.10165285>

7 AUTHORS

Sairul Izwan Safie received the Bachelor of Engineering (Electrical) and Master of Electrical Engineering (Power) from the Universiti Teknologi Malaysia. He received Ph.D. in Electronic and Electrical Engineering from the University of Strathclyde, Glasgow, United Kingdom. He is currently an Associate Professor of Universiti Kuala Lumpur – Malaysian Institute of Industrial Technology. His research interest lies in artificial intelligence, big data, signal and image processing with application to biometric, psychological and physiological signal, image and video processing (E-mail: sairulizwan@unikl.edu.my).

Noor Huda Ja'afar received B.E, M.E and PhD degrees in Electrical Engineering from Universiti Tun Hussein Onn Malaysia (UTHM). She is currently working as a Senior Lecturer at the Instrumentation and Control Engineering Section, Universiti Kuala Lumpur – Malaysian Institute of Industrial Technology. Her research interest includes 3D transformation, image processing, and reconfigurable computing (E-mail: noorhuda.jaafar@unikl.edu.my).

Azyyati Johari is currently holding an academic position in Universiti Kuala Lumpur – Malaysian Institute of Industrial Technology. She received the Bach. of Chemical Engineering (Hons) and Master in Chemical Engineering from Universiti Malaysia Pahang. Her research interest is in nanomaterial development for wireless application, chemical process plant optimization, wastewater treatment, and green technology (E-mail: azyyati@unikl.edu.my).

Mohd Anuar Ismail currently serves as a Senior Lecturer in the Plant Engineering Technology Section at Universiti Kuala Lumpur (UNIKL MITEC) in Pasir Gudang, Johor. He holds a PhD in Engineering (Precision Metrology & Inspection) from the University of Warwick, United Kingdom. His research interests include metrology and inspection instruments, additive manufacturing measurement, and the application of artificial intelligence and vibration analysis for plant condition-based maintenance (E-mail: manuar@unikl.edu.my).